

# Adiabaticity in nonreciprocal Landau-Zener tunneling

Wen-Yuan Wang<sup>1,2</sup> and Jie Liu<sup>3,4\*</sup>

<sup>1</sup>Key Laboratory of Atomic and Molecular Physics & Functional Materials of Gansu Province, College of Physics and Electronic Engineering, Northwest Normal University, Lanzhou 730070, China

<sup>2</sup>Beijing Computational Science Research Center, Beijing 100193, China

<sup>3</sup>Graduate School, China Academy of Engineering Physics, Beijing 100193, China

<sup>4</sup>HEDPS, Center for Applied Physics and Technology, and College of Engineering, Peking University, Beijing 100871, China

We investigate the Landau-Zener tunneling (LZT) of a self-interacting two-level system in which the coupling between the levels is nonreciprocal. In such a non-Hermitian system, when we adjust the energy bias between two levels very slowly, i.e., in the adiabatic limit, we find that a quantum state can still closely follow the eigenstate solution until it encounters the exceptional points (EPs), at which two eigenvalues and their corresponding eigenvectors coalesce. In the absence of the nonlinear self-interaction, we can obtain explicit expressions of the eigenvectors and eigenvalues and analytically deduce the adiabatic LZT probability according to invariant values at EPs. In the presence of the nonlinear interaction, the dynamics of the adiabatic evolutions are explicitly demonstrated with the help of classical trajectories in the plane of two reduced variables associated with the population difference and relative phase. We surprisingly find that the nonzero adiabatic tunneling probabilities cannot be correctly predicted by the classical action at EPs. We finally plot a phase diagram for large ranges of nonreciprocity and nonlinear interaction parameters to explicitly demonstrate where adiabaticity breaks down. Our theory is certified by numerical results, and important implications are discussed.

## I. INTRODUCTION

Landau-Zener tunneling (LZT) is one of the most fundamental models in the textbooks of quantum mechanics, which describes a system that goes from one side of an avoided level crossing to the other side at a certain sweeping rate [1, 2]. The LZT model has many important applications in various physical systems that is demonstrated by recent progress such as in superconducting qubits [3–5], nitrogen-vacancy centers [6], quantum dots [7, 8], waveguide arrays [9], and Bose-Einstein condensates [10–27], to name only a few.

The LZT model has many extensions by taking diverse physical conditions into account, such as in multilevel systems [28–36], in a nonlinear interacting system with level energies depending on the occupation of the levels [10–12], and in a time-dependent sweeping scheme [37, 38]. All the above studies focus on Hermitian systems, which are under the assumption of being conservative, obeying time-reversal symmetry, and obviously exhibiting real-valued eigenvalues. However, in many situations, nonconservative elements ubiquitously arise in various forms, and non-Hermitian physics have recently attracted considerable attention [39–45]. Recently, the extensions of the LZT to non-Hermitian systems are also studied by considering level decay and dephasing effect [46–48].

In the present paper, we attempt to investigate the LZT in a nonreciprocal self-interacting two-level system, in which the non-Hermitian is induced by the nonreciprocal coupling between levels in contrast to the level decay and dephasing effects [46–48]. The nonreciprocity of state transitions can be harnessed to engineer an effective non-Hermitian Hamiltonian [44, 45, 49, 50], which maintains the time-reversal symmetry but violates the parity symmetry. The Bogoliubov-de Gennes equation that describes the dynamics of noncondensed atoms in Bose-Einstein condensate [51–53], has this symmetry.

Such an idea has been used to realize a non-Hermitian Su-Schrieffer-Heeger model with asymmetric intra-unit-cell hopping amplitudes [54]. Nonreciprocity plays important roles not only in fundamental studies such as topological photonics [55, 56] and chiral quantum optics [57] but also in application research such as optical communication and information processing [58–61]. Recently, tunable nonreciprocal hopping has been realized in cold atoms in optical lattices [44, 62, 63] and in synthetic momentum lattices [64].

Additionally, quantum adiabatic evolution is an important concept in quantum mechanics [65, 66], which has been widely applied in the preparation and control of quantum states [67–70]. According to the adiabatic theorem of quantum mechanics, an initial nondegenerate eigenstate remains an instantaneous eigenstate if a Hamiltonian is changed sufficiently slowly compared to the level spacings. Adiabatic theory has been extended to quantum systems with nonlinear interactions [16, 71], showing many applications [72–74]. Recently, in the context of non-Hermitian systems, there are a few studies on possible new phenomena of adiabatic evolutions [70, 75–77]. In this paper, we address this issue by investigating an extended LZT model with nonreciprocal coupling, emphasizing the interplay of nonreciprocity and nonlinear interactions on adiabatic evolution. Interestingly, as we control the level bias in such a two-level system, the emergence of exceptional point (EP) singularities dramatically alters the tunneling process, leading to breakdown of adiabaticity. Our results are of significance in the fields of quantum optics and quantum transport. They also have potential application in quantum devices for quantum information.

The paper is organized as follows. In section II, we introduce the physical model of nonreciprocal LZT. In section III, we study the nonreciprocal LZT in the absence of nonlinear interactions. In section IV, in the adiabatic limit, we study the nonreciprocal LZT in the presence of nonlinear interactions. A summary is presented in section V.

\* E-mail address: [jliu@gscaep.ac.cn](mailto:jliu@gscaep.ac.cn).

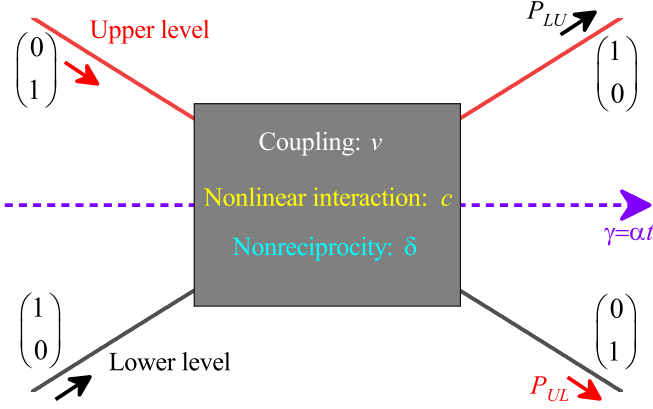


FIG. 1. (color online) Schematic illustration of nonreciprocal LZT based on a two-level system with nonlinear interactions. The two solid curves (red and black) represent the adiabatic energy levels (upper and lower levels, respectively). The shadow box represents the region in which the two levels closely approach each other and quantum tunneling emerges due to the complicated interplay between nonreciprocal coupling and nonlinear interactions. The level bias varies linearly in time as  $\gamma = \alpha t$  ( $\alpha$  is the so-called sweeping rate). Assuming that the system is initially on the lower (upper) energy level, the transition probability from the lower (upper) to the upper (lower) level during the sweeping process is denoted by  $P_{LU}$  ( $P_{UL}$ ).  $(1, 0)^T$  (or  $(0, 1)^T$ ) represents the eigenstate when  $\gamma \rightarrow \pm\infty$ .

## II. THE MODEL

We consider a nonreciprocal Landau-Zener model as illustrated by Fig. 1, whose Hamiltonian takes the following form:

$$H(\gamma) = \begin{pmatrix} \frac{\gamma}{2} + \frac{c}{2}(|b|^2 - |a|^2) & \frac{v}{2} \\ \frac{v}{2}(1 - \delta) & -\frac{\gamma}{2} - \frac{c}{2}(|b|^2 - |a|^2) \end{pmatrix}, \quad (1)$$

where  $(a, b)$  is the two-mode wavefunction,  $v$  is the hopping constant between the two levels,  $\gamma$  is the level bias,  $c$  denotes the nonlinear self-interaction parameter indicating the population-dependent level energy, and  $\delta > 0$  is the nonreciprocity parameter that might result in non-Hermiticity. Since the Hamiltonian can be scaled by dividing by  $v$ , for convenience, we can set  $v = 1$  as the energy unit hereafter.

The dimensionless Schrödinger equation is  $i \frac{d}{dt} \begin{pmatrix} a \\ b \end{pmatrix} = H(\gamma) \begin{pmatrix} a \\ b \end{pmatrix}$ . Since Hamiltonian (1) is non-Hermitian, the distinct feature is the appearance of complex eigenvalues. Thus, the time evolution of such a non-Hermitian system is no longer unitary. To study the probability distribution and expectation value of an observable, one should normalize the time-dependent amplitudes  $a(t)$  and  $b(t)$  by the total population  $N(t)$ . As in the standard Landau-Zener model, we take  $v$  to be independent of time and the level bias  $\gamma$  to be a tunable control parameter; hence,  $\gamma$  changes linearly with time as  $\gamma = \alpha t$ . The constant rate  $\alpha$  is the sweeping rate.

The wavefunction can be expressed in its amplitude and phase by  $a = n_a e^{i\theta_a}$  and  $b = n_b e^{i\theta_b}$ , and the Schrödinger equation

is cast into the following form:

$$\dot{n}_a = \frac{v}{2} n_b \sin(\theta_b - \theta_a), \quad (2a)$$

$$\dot{n}_b = -\frac{v}{2} (1 - \delta) n_a \sin(\theta_b - \theta_a), \quad (2b)$$

$$\dot{\theta}_a = -\frac{\gamma}{2} - \frac{c}{2} (n_b^2 - n_a^2) - \frac{v}{2} \frac{n_b}{n_a} \cos(\theta_b - \theta_a), \quad (2c)$$

$$\dot{\theta}_b = \frac{\gamma}{2} + \frac{c}{2} (n_b^2 - n_a^2) - \frac{v(1 - \delta)}{2} \frac{n_a}{n_b} \cos(\theta_b - \theta_a). \quad (2d)$$

In the absence of nonreciprocity  $\delta$  and nonlinear interaction  $c$ , Hamiltonian (1) degenerates into a standard linear LZT two-level system. The transition probability between the two energy levels is represented by the formula [1, 2]  $P_{LZ} = \exp\left(-\frac{\pi v^2}{2\alpha}\right)$ . In the adiabatic limit, that is, as the sweeping rate  $\alpha$  tends to zero, the transition probability tends to zero, indicating that an initial quantum state can closely follow the instantaneous eigenstate and remain on the adiabatic (upper or lower) energy level.

The presence of a nonlinear interaction  $c$  can dramatically alter the tunneling dynamics [10–27]. The most striking feature is the breakdown of adiabaticity for a large nonlinear parameter, which is intimately linked to the hysteretic phenomena and the existence of swallowtail loops in the adiabatic energy levels [10, 12, 13, 16, 78]. The underlying mechanism has been revealed by investigating an equivalent classical Hamiltonian, in which the nonzero adiabatic tunneling probability can be explained as a jump in the classical canonical action [12, 16].

The presence of nonreciprocity parameter  $\delta$  in Hamiltonian (1) can result in nonreciprocal state transitions between two levels. In contrast to  $\mathcal{PT}$ -conserved non-Hermitian systems [39], this non-Hermitian system maintains the time-reversal symmetry but violates the parity symmetry. In the following sections, we will investigate distinct features of its tunneling dynamics and adiabaticity induced by the nonreciprocal transitions of quantum states.

## III. NONRECIPROCAL LZT IN THE ABSENCE OF NONLINEAR INTERACTIONS

### A. Energy level and nonreciprocal LZT

When  $c = 0$ , the eigenvalues and eigenstates of Hamiltonian (1) can be readily obtained. The adiabatic levels are given by

$$\varepsilon_{\pm} = \pm \frac{1}{2} \sqrt{\gamma^2 + v^2(1 - \delta)}. \quad (3)$$

The corresponding adiabatic eigenstates are given by

$$\begin{aligned} |\varepsilon_{-}\rangle &= \left\{ \frac{\gamma - \sqrt{\gamma^2 + v^2(1 - \delta)}}{v(1 - \delta)}, 1 \right\}, \\ |\varepsilon_{+}\rangle &= \left\{ \frac{\gamma + \sqrt{\gamma^2 + v^2(1 - \delta)}}{v(1 - \delta)}, 1 \right\}. \end{aligned} \quad (4)$$

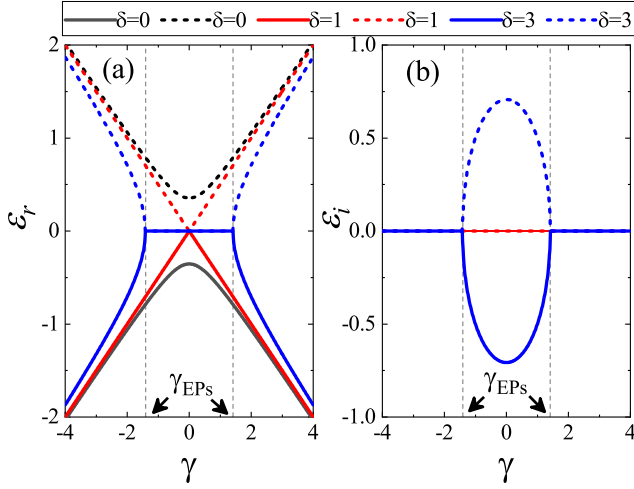


FIG. 2. (color online) Adiabatic levels  $\varepsilon$  versus bias  $\gamma$  for different nonreciprocity parameters  $\delta = 0$  (black curve), 1 (red curve), and 3 (blue curve). (a) and (b) present the real and imaginary parts of adiabatic levels, respectively. For  $\delta \leq 1$ , the imaginary parts of energy are always 0, and they overlap in (b). For  $\delta > 1$ , with increasing  $\gamma$ , EPs occur at  $\pm\gamma_{EPs}$ , and the corresponding eigenvalues coalesce. In both (a) and (b), the dashed magenta lines mark the location of EPs.

EPs are a distinct feature in quantum systems, at which two eigenvalues and their corresponding eigenvectors coalesce and become degenerate. For nonreciprocity parameter  $\delta \geq 1$ , the conditions for EPs can be easily obtained, that is,  $\gamma_{EPs} = \pm\sqrt{\delta-1}$ . The eigenvalues are real when  $|\gamma| > |\gamma_{EPs}|$ ; otherwise, they are imaginary. The corresponding eigenvectors at EPs coalesce as

$$|\varepsilon_{EP}\rangle = \left\{ \mp \frac{1}{\sqrt{\delta}}, \frac{\sqrt{\delta-1}}{\sqrt{\delta}} \right\}, \quad (5)$$

where the sign  $\mp$  is for the  $\pm\gamma_{EPs}$  EPs, respectively. For nonreciprocity parameter  $\delta < 1$ , there are no EPs, and the eigenvalues are always real.

The level bias  $\gamma$ -dependence of the energy levels is shown in Fig. 2. When  $\delta < 1$ , the imaginary parts of eigenvalues are always zero, and the real parts of eigenvalues show an avoided level crossing at  $\gamma = 0$ . For  $\delta = 1$ , the eigenvalues show a level crossing at  $\gamma = 0$ . For  $\delta > 1$ , with increasing  $\gamma$ , EPs occur at  $\gamma_{EPs}$ , and the corresponding eigenvalues coalesce. Between two EPs, the real parts of the eigenvalues are zero, whereas the imaginary parts of the eigenvalues are nonzero.

Note that the corresponding eigenstates are not orthogonal to each other. For  $\gamma \rightarrow \pm\infty$ ,  $\varepsilon \rightarrow \pm|\gamma|/2$ . For instance, on the lower level, we have  $(a, b) \rightarrow (1, 0)$  at  $\gamma \rightarrow -\infty$  and  $(a, b) \rightarrow (0, 1)$  at  $\gamma \rightarrow +\infty$ .

We now focus on the nonreciprocal LZT. The numerical results of the tunneling probability for different sweeping rates  $\alpha$  and nonreciprocity parameters  $\delta$  are shown in Fig. 3. Figures 3(a) and (b) show the tunneling probabilities  $P_{LU}$  and  $P_{UL}$ , respectively, as a function of the sweeping rate  $\alpha$  for different nonreciprocity parameters  $\delta = 0, 0.5, 1$ , and 3. For  $\delta = 0$ , both the tunneling probabilities  $P_{LU}$  and  $P_{UL}$  are consistent with the standard formula of the LZT probability. For  $\delta \neq 0$ ,

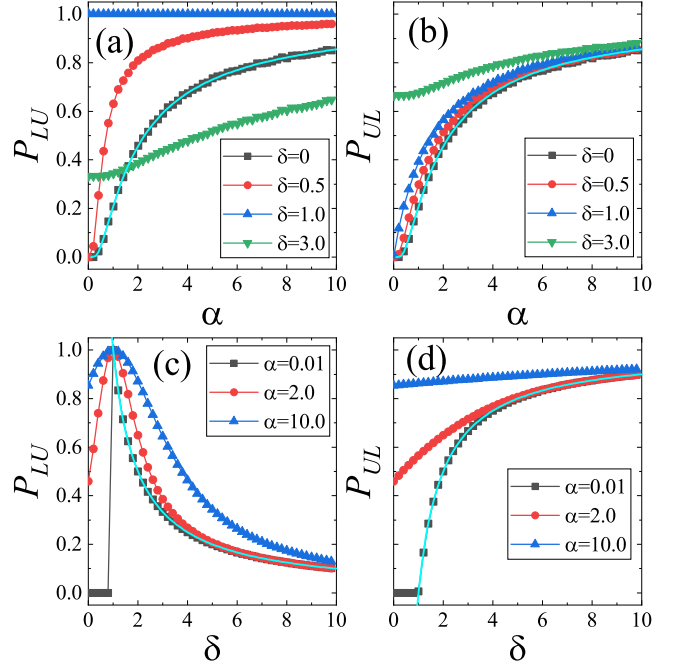


FIG. 3. (color online) Nonreciprocal LZT probability. (a) and (b) present the tunneling probabilities  $P_{LU}$  and  $P_{UL}$ , respectively, as a function of sweeping rate  $\alpha$  for different nonreciprocity parameters  $\delta = 0, 0.5, 1$ , and 3. (c) and (d) present the tunneling probabilities  $P_{LU}$  and  $P_{UL}$ , respectively, as a function of nonreciprocity parameter  $\delta$  for different sweeping rates  $\alpha = 0.01, 2$ , and 10. In both (a) and (b), the cyan curve indicates the standard LZT probability. The cyan curves in (c) and (d) indicate the functions with forms of  $1/\delta$  and  $(\delta-1)/\delta$ , respectively.

nonreciprocity greatly changes the LZT, resulting in obvious breaking of the symmetry in the tunneling between the two levels, i.e.,  $P_{LU} \neq P_{UL}$ . For  $\delta = 0.5$ , both the tunneling probabilities  $P_{LU}$  and  $P_{UL}$  exponentially increase as  $\alpha$  increases. For  $\delta = 1$ , with the increase in  $\alpha$ , the tunneling probability  $P_{LU}$  remains 1, whereas the tunneling probability  $P_{UL}$  exponentially increases. For  $\delta = 3$ , both the tunneling probabilities  $P_{LU}$  and  $P_{UL}$  nonexponentially increase as  $\alpha$  increases. For subcritical values of the nonreciprocity parameter  $\delta < 1$ , the tunneling probability still exponentially vanishes with  $\alpha$ . Most strikingly, both of the tunneling probabilities  $P_{LU}$  and  $P_{UL}$  for  $\delta > 1$  are not zero in the adiabatic limit  $\alpha \rightarrow 0$ , while they are zero for  $\delta < 1$ . This shows that  $\delta = 1$  is the critical point for the adiabatic transition.

Figures 3(c) and (d) more clearly depict the tunneling probabilities  $P_{LU}$  and  $P_{UL}$ , respectively, as a function of the nonreciprocity parameter  $\delta$  for different sweeping rates  $\alpha = 0.01, 2$ , and 10. In the adiabatic limit, i.e.,  $\alpha = 0.01$ , both the tunneling probabilities  $P_{LU}$  and  $P_{UL}$  remain zero when  $\delta < 1$ . At  $\delta = 1$ ,  $P_{LU}$  quickly reaches 1, whereas  $P_{UL}$  remains 0. For  $\delta > 1$ , with increasing  $\delta$ ,  $P_{LU}$  decreases as a function with the form of  $1/\delta$ , and  $P_{UL}$  increases as a function with the form of  $(\delta-1)/\delta$ . In the nonadiabatic cases, i.e.,  $\alpha = 2, 10$ , as  $\delta$  increases from 0 to 1,  $P_{LU}$  continuously increases. When  $\delta = 1$ ,  $P_{LU}$  reaches the saturation value of 1 regardless of  $\alpha$ ; then, as  $\delta$  continues to increase,  $P_{LU}$  keeps decreasing. When

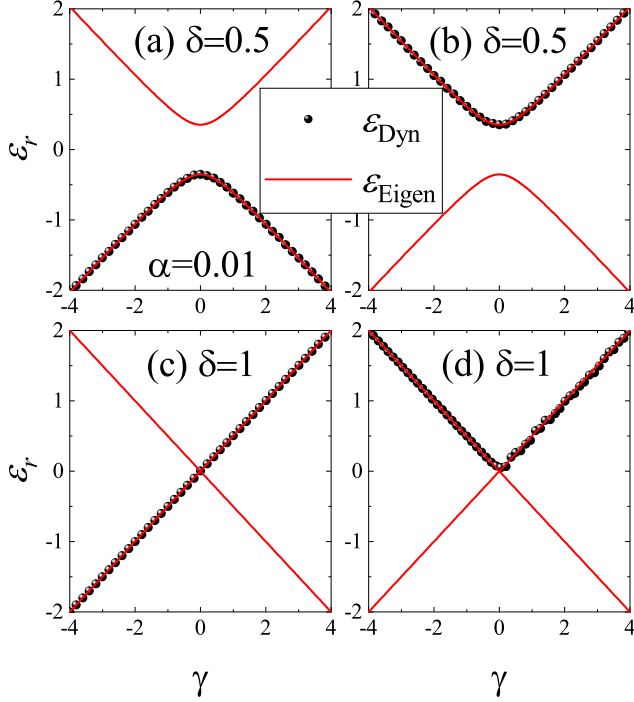


FIG. 4. (color online) Comparison of the dynamical levels  $\varepsilon_{\text{Dyn}}$  (circles) and the adiabatic levels  $\varepsilon_{\text{Eigen}}$  (solid lines) for  $\delta \leq 1$ . (a) and (b) present the results for  $\delta = 0.5$ , and (c) and (d) present the results for  $\delta = 1$ . For dynamical evolution, we take the adiabatic limit of  $\alpha = 0.01$  as an example.

$\delta$  reaches a sufficiently large value,  $P_{LU}$  decreases to 0. In the nonadiabatic cases,  $P_{UL}$  increases as  $\delta$  increases.

From the above, we strikingly find that even in the adiabatic limit  $\alpha \rightarrow 0$ , the tunneling probability can take nonzero values, which solely depends on the nonreciprocity parameter in the forms of  $1/\delta$  and  $(\delta - 1)/\delta$ , as indicated by the cyan curves in Figs. 3(c) and 3(d). In other words, nonreciprocity can break the adiabaticity of quantum evolutions.

### B. Nonreciprocity breaks adiabaticity

To gain insight into the adiabaticity in nonreciprocal LZT, we calculate the dynamical energy in the temporal evolution. For a normalized dynamic state  $|\psi(t)\rangle = (a(t), b(t))^T$ , the dynamical energy can be obtained by calculating the energy expectation values of the dynamic states,

$$\varepsilon_{\text{Dyn}} = \langle \psi(t) | H(\gamma = \alpha t) | \psi(t) \rangle. \quad (6)$$

A comparison of the dynamical levels  $\varepsilon_{\text{Dyn}}$  and the adiabatic levels  $\varepsilon_{\text{Eigen}}$  is shown in Fig. 4. Figures 4(a) and (b) show the results for  $\delta = 0.5$ , and (c) and (d) show those for  $\delta = 1$ . The initial state is prepared in the lower level (i.e.,  $(a, b) = (1, 0)$ ) for Figs. 4(a) and (c) and in the upper level (i.e.,  $(a, b) = (0, 1)$ ) for Figs. 4(b) and (d). The results are shown in Fig. 4 for the adiabatic limit with  $\alpha = 0.01$  as an example. In Figs. 4(a) and (b), where  $\delta = 0.5$ , we see an excellent match between the dynamical levels and the adiabatic levels, which is similar to the case of  $\delta = 0$  [10]. This

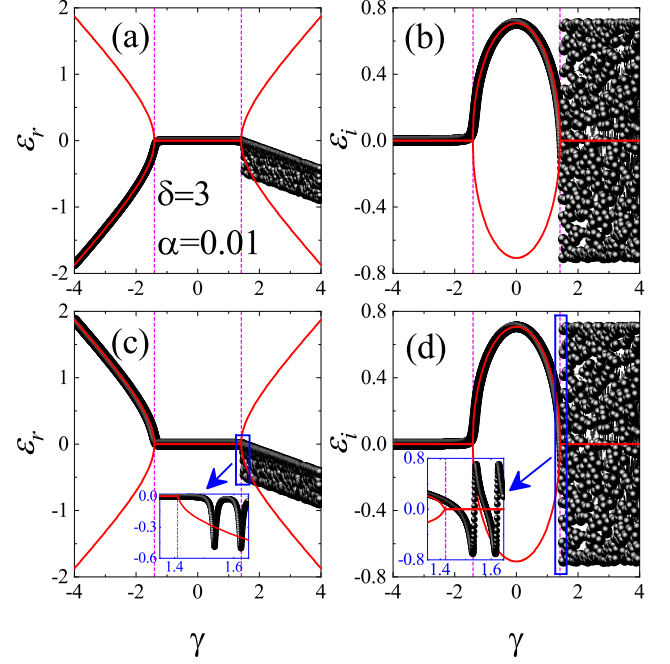


FIG. 5. (color online) Comparison of the dynamical levels  $\varepsilon_{\text{Dyn}}$  (circles) and the adiabatic levels  $\varepsilon_{\text{Eigen}}$  (solid lines) for  $\delta > 1$ . In this case, the EPs occur at  $\gamma = \gamma_{\text{EPs}}$ , which are marked by two magenta dotted lines. (a) and (c) present the real parts of the energy levels, and (b) and (d) present the imaginary parts of the energy levels. For dynamical evolution, the system is initially prepared in the lower adiabatic levels for (a) and (b), i.e.,  $(a, b) = (1, 0)$ , whereas the system is initially prepared in the upper adiabatic levels for (c) and (d), i.e.,  $(a, b) = (0, 1)$ . Here, we take  $\delta = 3$  and the adiabatic limit as  $\alpha = 0.01$  as an example.

demonstrates that for the case of  $\delta < 1$ , the quantum state can closely follow the corresponding eigenstates in the adiabatic evolution, indicating that adiabaticity is maintained.

At the critical value of  $\delta = 1$ , the upper level and lower level cross at  $\gamma = 0$ . We calculate the dynamical energy levels, shown in Figs. 4 (c) and (d). The results show that the initial state starting from both the upper level and lower level can finally evolve into the upper level. This is because the nonreciprocity parameter eliminates one of the channels in the hopping. When  $\delta = 1$ , the adiabatic levels of Hamiltonian (1) are given by  $\varepsilon_{\pm|\delta=1} = \pm \frac{1}{2}\gamma$ , and the corresponding adiabatic eigenstates are given by  $|\varepsilon_{-}\rangle_{\delta=1} = (-v/2\gamma, 1)$  and  $|\varepsilon_{+}\rangle_{\delta=1} = (1, 0)$ . For  $\gamma \rightarrow 0$ , both eigenvalues  $\varepsilon_{\pm|\delta=1} \rightarrow 0$  and their corresponding eigenvectors coalesce as  $|\varepsilon_{\pm}\rangle_{\delta=1} \rightarrow (1, 0)$ , indicating the appearance of an EP. After that, the dynamic state always follows the upper adiabatic eigenstates.

For  $\delta > 1$ , EPs occur at  $\gamma = \pm\gamma_{\text{EPs}}$ . Therefore, when  $\gamma$  changes from  $-\infty$  to  $+\infty$ , the system will pass through the EPs; here, the adiabaticity might break. A comparison of the dynamical levels  $\varepsilon_{\text{Dyn}}$  and the adiabatic levels  $\varepsilon_{\text{Eigen}}$  for  $\delta = 3$  is shown in Fig. 5. Figures 5(a) and (b) show the real part and imaginary part of the energy levels. We see that in the range of  $\gamma < \gamma_{\text{EPs}}$ , the initial state prepared in either the upper or lower level can perfectly follow the real part of the adiabatic energy level. However, in the range from  $-\gamma_{\text{EPs}}$  to  $+\gamma_{\text{EPs}}$ , both



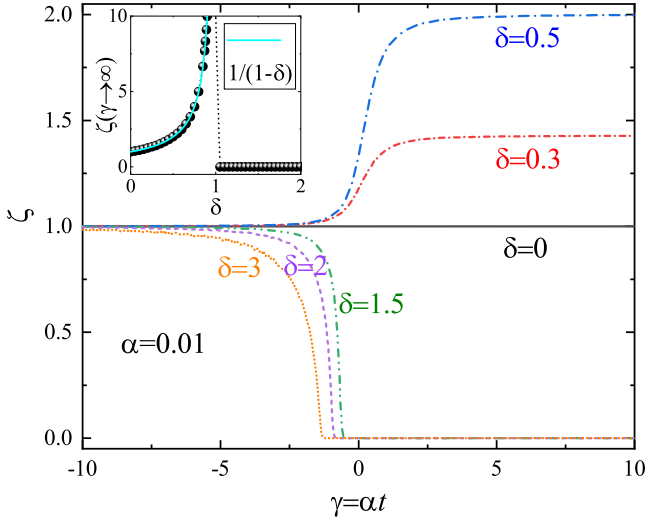


FIG. 6. (color online) In the adiabatic limit (i.e.,  $\alpha = 0.01$ ), normalized invariant values  $\zeta$  as a function of  $\gamma = \alpha t$  for different  $\delta$ . Inset:  $\zeta$  as a function of nonreciprocity parameter  $\delta$  for  $\gamma \rightarrow \infty$ .

states evolve following the imaginary part of the upper level. This is due to the so-called skin effect [45], in which, in the non-Hermitian system, the eigenstate with a real imaginary part will dominate the dynamical evolution. More interestingly, when  $\gamma > +\gamma_{EPs}$ , the quantum states follow neither the upper level nor the lower level, clearly indicating breakdown of adiabaticity.

Now, we reveal the underlying mechanism of the breakdown of adiabaticity, and we first deduce the following relations from Eq. (2):

$$\zeta = n_a^2 - \frac{1}{(\delta - 1)} n_b^2, \quad (7a)$$

$$\dot{N} = v\delta n_a n_b \sin \theta, \quad (7b)$$

$$\dot{\theta} = \gamma + \frac{v}{2} \frac{n_b^2 - (1 - \delta)n_a^2}{n_a n_b} \cos \theta. \quad (7c)$$

In Fig. 6, we plot the normalized  $\zeta$  (i.e., divided by  $N$  in each integration step) as a function of  $\gamma = \alpha t$  for various  $\delta$ . Clearly,  $\zeta$  starting from 1 always converges to a certain constant value for large  $\gamma$ . In the case of reciprocity (i.e.,  $\delta = 0$ ),  $\zeta$  remains at 1. This is because the evolution in this case is unitary, and  $\zeta$  is a conserved quantity. In the weak nonreciprocal regime ( $\delta < 1$ ),  $\zeta$  converges to a nonzero value, which is solely determined by the nonreciprocity parameter in the simple form of  $-1/(\delta - 1)$  (as shown in the inset in Fig. 6). The reason is that, for the case of  $\delta < 1$ , the adiabaticity is maintained such that the quantum state keeps evolving on the lower level and finally reaches  $(n_a, n_b) = (0, 1)$  for large positive  $\gamma$ ; that is,  $\zeta$  tends to  $-1/(\delta - 1)$ .

In the strong nonreciprocal regime ( $\delta > 1$ ), we interestingly find that after EPs,  $\zeta$  remains the constant value of zero regardless of  $\delta$ . This is because, considering the explicit expression Eq. (5) of the wavefunctions at EPs, after EPs, Eq.

(7) becomes

$$0 = n_a^2 - \frac{1}{(\delta - 1)} n_b^2, \quad (8a)$$

$$\dot{N} = v\sqrt{\delta - 1} \sin \theta, \quad (8b)$$

$$\dot{\theta} = \gamma + v\sqrt{\delta - 1} \cos \theta. \quad (8c)$$

Using Eq. (8a) and considering the normalization relation, we can finally obtain the adiabatic tunneling probability

$$P_{LU}^{ad} = \frac{1}{\delta}, \quad P_{UL}^{ad} = 1 - \frac{1}{\delta}, \quad (\delta \geq 1). \quad (9)$$

The above analytic expressions are in full agreement with the numerical results, as shown in Figs. 3(c) and (d).

#### IV. ADIABATICITY OF NONRECIPROCAL LZT IN THE PRESENCE OF NONLINEAR INTERACTIONS

We introduce two reduced variables  $s = n_b^2 - n_a^2$  and  $\theta = \theta_b - \theta_a$ , which are associated with the population difference and relative phase. In terms of  $s$  and  $\theta$ , the nonreciprocal nonlinear equations of (2) are then reduced to the following motion equations:

$$\dot{s} = \frac{v}{2}(\delta - 2)\sqrt{1 - s^2} \sin \theta, \quad (10a)$$

$$\dot{\theta} = \gamma + cs + \frac{v[(1 + s) - (1 - \delta)(1 - s)]}{2\sqrt{1 - s^2}} \cos \theta. \quad (10b)$$

Note that the above equations do not correspond to a conservative Hamiltonian system [79] due to  $\frac{\partial \dot{s}}{\partial s} - \frac{\partial \dot{\theta}}{\partial \theta} \neq 0$ .

To investigate the adiabaticity, we need to analyze the behavior of the adiabatic levels in the nonlinear model. These levels are the solution of the time-independent version of the Schrödinger equation obtained by replacing  $i\partial/\partial t$  with the energy  $\varepsilon$ , i.e.,  $\varepsilon \begin{pmatrix} a \\ b \end{pmatrix} = H(\gamma) \begin{pmatrix} a \\ b \end{pmatrix}$ . By using the constraint of  $n_a^2 + n_b^2 = 1$ , we find that the eigenenergy  $\varepsilon$  satisfies the following quartic equation:

$$\varepsilon^4 + c\varepsilon^3 + A\varepsilon^2 + B\varepsilon + D = 0, \quad (11)$$

where  $A = [4c^2 - 4\gamma^2 - v^2(4 - 4\delta - \delta^2)]/16$ ,  $B = cv^2(\delta - 1)/4$ , and  $D = [-c^2v^2(4 - 4\delta + \delta^2) + 2cv^2\delta\gamma(2 - \delta) - v^2\delta^2(\gamma^2 + v^2 - v^2\delta)]/64$ . When  $\delta = 0$ , the above equation reduces to that of [10]. This quartic equation may only have two pure real roots for small reciprocity parameter and nonlinear parameter; approximately, we estimate  $c < v\sqrt{1 - \delta}$ . Otherwise, it may have four real roots in a certain range of  $\gamma$ , leading to the emergence of EPs, as shown below. We focus on the situation in which the initial state is prepared in the lower level and attempt to investigate its adiabatic evolution in the limit of  $\alpha \rightarrow 0$ .

##### A. In the weak nonreciprocal regime ( $\delta < 1$ )

We now focus on adiabaticity in the weak nonreciprocal regime, i.e.,  $\delta < 1$ . We numerically calculate the real and

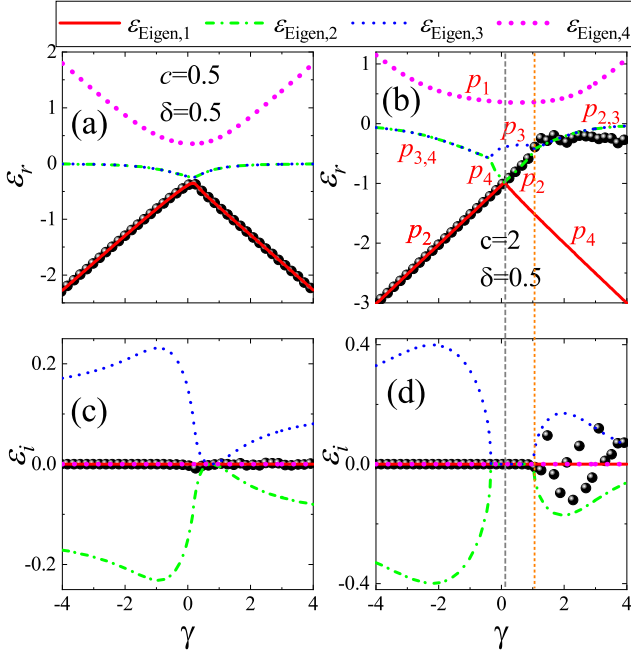


FIG. 7. (color online) In the presence of nonlinear interactions and in the weak nonreciprocal regime, i.e.,  $\delta = 0.5$ , dynamical levels  $\varepsilon_{\text{Dyn}}$  (circles) and adiabatic levels  $\varepsilon_{\text{Eigen}}$  (solid lines). (a) and (c) present the real part and imaginary part of the energy levels for  $c = 0.5$ . (b) and (d) present the real part and imaginary part of the energy levels for  $c = 2$ . For dynamical evolution, the system is initially prepared in the lower adiabatic levels, i.e.,  $(a, b) = (1, 0)$ . Here, the dynamic evolution is in the adiabatic limit ( $\alpha = 0.01$ ). In (b),  $p_i$  are the fixed points shown in Fig. 8, which correspond to the eigenstates of the energy level.

imaginary parts of the energy levels. In Figs. 7(a) and (c), for a small nonlinearity of  $c = 0.5$ , we see that in addition to the two pure real energy levels (maximum and minimum), there are two complex energy levels whose values are conjugate pairs. We obtain the dynamical energy levels of the system evolved from  $(a, b) = (1, 0)$ , shown in Fig. 7. In Figs. 7(a) and (c), we see an excellent match between the dynamical levels and the adiabatic levels for both the real and imaginary parts of the energy levels.

For the large nonlinearity of  $c = 2$ , we find in Figs. 7(b) and (d) that the energy levels have a dramatic change: there are four pure real energy levels in a window near  $\gamma = 0$ , where a loop appears. Notably, for reciprocal systems, the appearance of a loop breaks the adiabaticity [10–13, 16, 78]. The primary mechanism for the breakdown of adiabaticity is that when the state moves up to the edge of the loop, there is no way to go any further except to jump to the upper and lower levels [10]. However, for the nonreciprocal system we consider here, as shown in Figs. 7(b) and (d), eigenenergies still exist in the conjugate pair  $(p_2$  and  $p_3)$  beyond the edge of the loop. Nevertheless, the dynamical evolution does not follow these eigenlevels.

To clearly analyze adiabatic dynamics in the presence of nonlinear interactions, in Fig. 8, we show the evolution of the classical trajectories in the plane of two reduced variables  $(s, \theta)$  as  $\gamma$  adiabatically changes. In the plane of  $(s, \theta)$ , the

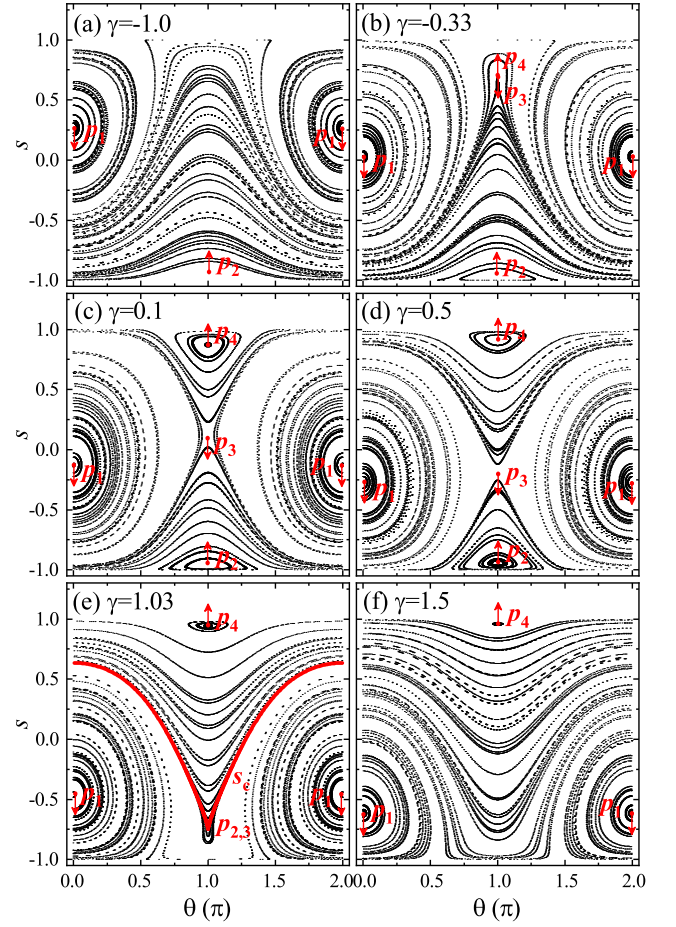


FIG. 8. (color online) Evolution of the classical trajectories in the plane of two reduced variables  $(s, \theta)$  for some typical values of  $\gamma$ . Here, we take  $c = 2$  and  $\delta = 0.5$  as examples. The dots and bold red line indicate the fixed points. The arrows indicate the shifting direction of the fixed points  $p_i$  as  $\gamma$  increases. The curves are the periodic trajectories. In (c), we take  $\gamma = 0.1$ , which corresponds to the position of  $\gamma$  identified by the dashed line in Fig. 7(b). In this case, four fixed points occur, implying that four eigenstates do not coalesce. In (e), we take  $\gamma = 1.03$ , which corresponds to the terminal point of the loop (as marked by the dotted line in Fig. 7(b)). In this case, the fixed points  $p_2$  and  $p_3$  merge to form a new homoclinic orbit  $s_c$ , implying that these two eigenstates coalesce.

fixed points of motion equations (10) correspond to the eigenstates that can be obtained by equating the right-hand sides of Eqs. (10)(a) and (b) to zero. At the terminal point of the loop, two fixed points merge (as shown in Figs. 8(b) and (e)), indicating that the corresponding eigenstates coalesce. The terminal points of the loop are indeed EPs, which can break the adiabaticity of dynamical evolution.

In Refs. [12, 16], the adiabatic evolution of the fixed points as a function of level bias was proven to correspond to the adiabatic evolution of the eigenstates. Breakdown of adiabaticity occurs when two fixed points merge together and form a homoclinic orbit. The nonzero adiabatic tunneling probability can then be calculated from the nonzero classical canonical action ( $I_c = \frac{1}{2\pi} \int_0^{2\pi} s d\theta$ ) of the homoclinic orbit as  $p_c^{ad} = I_c/2$ . In Fig. 9, we show the adiabatic tunneling probabilities  $p_{LU}^{ad}$

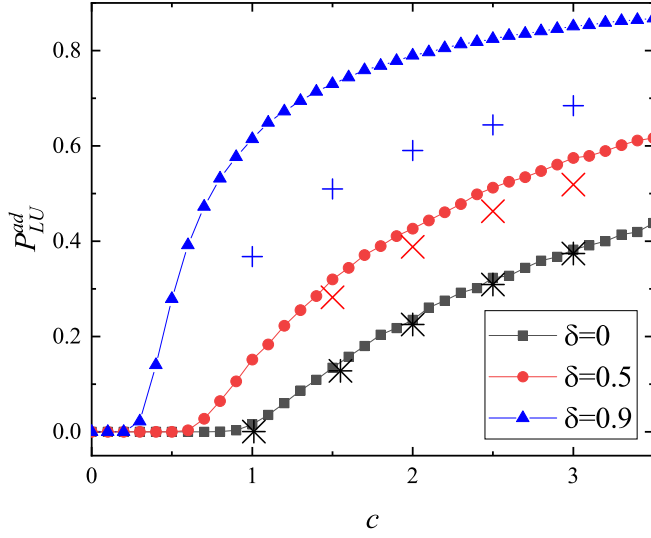


FIG. 9. (color online) Comparison of the adiabatic tunneling probability  $p_{LU}^{ad}$  (solid symbols) obtained by directly integrating the time-dependent nonlinear Schrödinger equation and  $p_c^{ad} = I_c/2$  (cross symbols) calculated from the classical canonical action ( $I_c$ ) of the homoclinic orbit at an EP.

obtained by directly integrating the time-dependent nonlinear Schrödinger equation and compare them with the  $p_c^{ad} = I_c/2$  calculated from the classical canonical action ( $I_c$ ) of the homoclinic orbit at an EP. For  $\delta = 0$ , they agree very well with each other. For a small nonreciprocal parameter up to  $\delta = 0.5$ , they fairly match each other. With a further increase in the nonreciprocal parameter, the difference between them becomes apparent. In this case, the nonzero adiabatic tunnel-

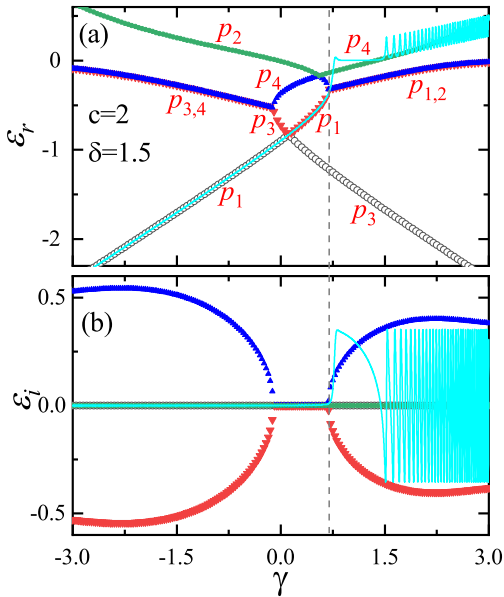


FIG. 10. (color online) In the strong nonreciprocal regime, i.e.,  $\delta = 1.5$ , dynamical levels  $\varepsilon_{\text{dyn}}$  (solid lines) and adiabatic levels  $\varepsilon_{\text{Eigen}}$  (circles). (a) and (b) present the real part and imaginary part of the energy levels. In (a),  $p_i$  are the fixed points shown in Fig. 11.

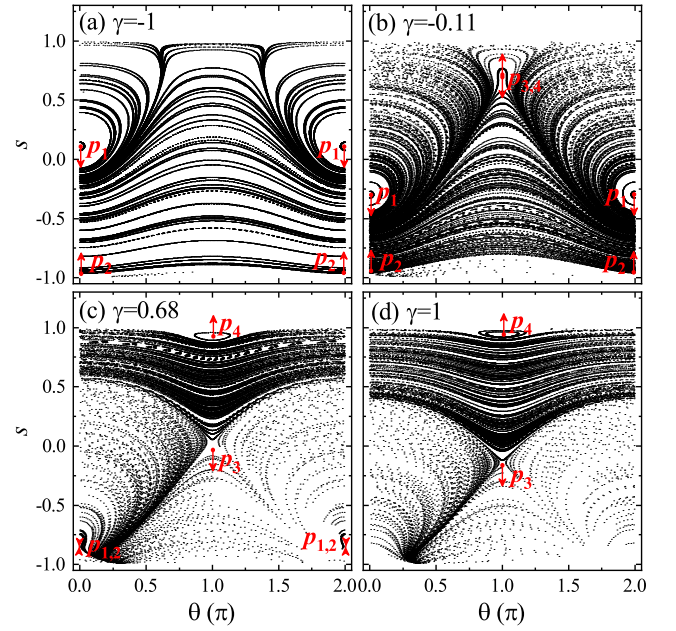


FIG. 11. (color online) In the strong nonreciprocal regime, i.e.,  $\delta = 1.5$ , evolution of the classical trajectories in the plane of two reduced variables ( $s, \theta$ ) for some typical values of  $\gamma$ . The dots indicate the fixed points, and the arrows indicate the shifting direction of the fixed points  $p_i$  as  $\gamma$  increases. The curves are the periodic trajectories. (a) For  $\gamma = -1$ , there are two fixed points  $p_1$  and  $p_2$  along the line  $\theta = 0$ . (b) For  $\gamma = -0.1$ , in addition to the two fixed points along the line  $\theta = 0$ , there are two fixed points  $p_3$  and  $p_4$  appearing along the line  $\theta = \pi$ . (c) For  $\gamma = 0.68$ , which corresponds to the position of  $\gamma$  identified by the dashed line in Fig. 10(b), the two fixed points  $p_1$  and  $p_2$  merge, implying that these two eigenstates coalesce. (d) For  $\gamma = 1$ , there are two fixed points  $p_3$  and  $p_4$  along the line  $\theta = \pi$ .

ing probabilities cannot be correctly predicted by the classical action at EPs. In fact, in the presence of nonreciprocity, the system of Eq. (10) is no longer a conserved Hamiltonian system.

### B. In the strong nonreciprocal regime ( $\delta > 1$ )

In the strong nonreciprocal regime, i.e.,  $\delta > 1$ , we numerically calculate the real and imaginary parts of the energy levels, and the results are shown in Fig. 10. In this case, the adiabatic levels are similar to those at  $\delta = 0.5$ , but the width of the parameter window with four pure real roots is narrowed. For adiabatic dynamical evolution, quantum states always follow adiabatic energy levels until the edge of the loop. After that, the dynamical evolution does not follow these eigenlevels.

In Fig. 11, we show the evolution of the classical trajectories in the plane of two reduced variables ( $s, \theta$ ) for some typical values of  $\gamma$ . At the terminal point of the loop, two fixed points  $p_1$  and  $p_2$  merge (as shown in Figs. 11(b) and (c)), indicating that these two eigenstates coalesce, leading to EPs. On the quantum state evolution path, the appearance of EPs will alter the adiabatic behavior of quantum state evolution, resulting in breakdown of adiabaticity.

In Fig. 12, we plot the normalized  $\zeta$  (i.e., divided by  $\mathcal{N}$  in

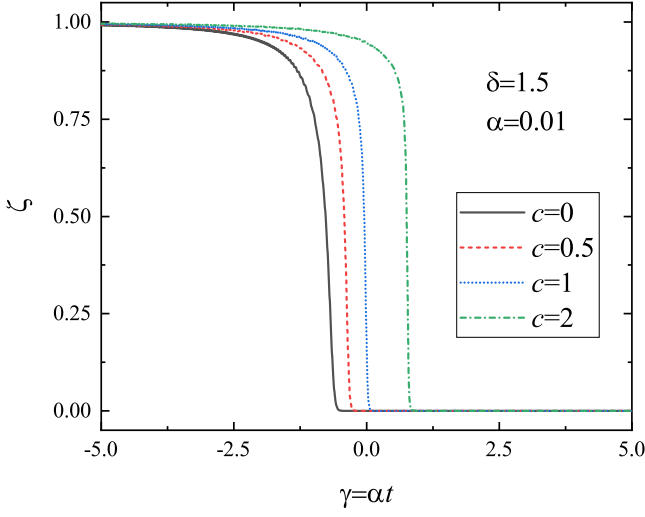


FIG. 12. (color online) In the strong nonreciprocal regime, i.e.,  $\delta = 1.5$ , normalized invariant values  $\zeta$  as a function of  $\gamma = \alpha t$  for different nonlinearities  $c$ .

each integration step) as a function of  $\gamma = \alpha t$  for various  $c$ . Clearly, in the strong nonreciprocal regime ( $\delta > 1$ ),  $\zeta$  starting from 1 finally converges to zero regardless of the values of  $c$  and  $\delta$ . Based on these observations, in the strong nonreciprocal regime, we can readily obtain the adiabatic LZT probability, which is consistent with the linear case shown in Eq. (9). This result is very interesting, implying that EPs induced by nonreciprocity can completely inhibit the nonlinear interaction effects.

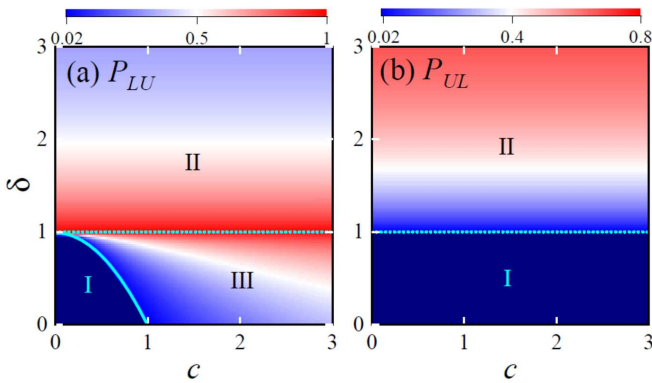


FIG. 13. (color online) Phase diagram of adiabaticity on the parameter plane ( $c$ ,  $\delta$ ). (a) and (b) correspond to  $P_{LU}$  and  $P_{UL}$ , respectively. I is the adiabaticity region. II is the breakdown of adiabaticity region induced by strong nonreciprocity. III is the breakdown of adiabaticity region where EPs are induced by the interplay between nonreciprocity and nonlinear interactions. Here, we still focus on the adiabatic limit and take the sweeping rate  $\alpha = 0.01$ . The cyan solid curve in (a) indicates the function with the form of  $\delta = 1 - c^2$ . The dashed lines in both (a) and (b) indicate the line  $\delta = 1$ .

### C. Phase diagram of adiabaticity

Figure 13 shows the phase diagram of adiabaticity for a large range of nonreciprocity and nonlinearity parameters, where panels (a) and (b) show the adiabatic transition probabilities  $P_{LU}$  and  $P_{UL}$ , respectively. There are three regions. I is the adiabaticity region, in which there are no EPs and the adiabatic evolution of quantum states remains. II is the regime of strong nonreciprocity, where the EPs not only break the adiabatic evolution of quantum states but also completely suppress the nonlinear interaction effect, resulting in the tunneling probabilities  $P_{LU}$  and  $P_{UL}$  taking the exact same form as that in the linear situation. Region III is the intermediate region, where EPs are induced by the interplay between nonreciprocity and nonlinear interactions. In this regime, for small nonreciprocity, the adiabatic tunneling probability can be approximately given by the classical action theory [12, 80], while when the nonreciprocity parameter tends to 1, the deviation between the theory and the numerical results becomes obvious. The boundary between regions I and III is determined by the emergence of the degenerate root of the quartic equation of Eq. (11) and can be estimated by  $c < \sqrt{1 - \delta}$ .

### V. CONCLUSION

In this work, we numerically and analytically investigate adiabaticity in the nonreciprocal Landau-Zener model with a nonlinear self-interaction. In this model, hopping nonreciprocity can lead to non-Hermiticity, which is distinct from the  $\mathcal{PT}$  system, whose non-Hermiticity is induced by a complex onsite potential. In the adiabatic limit of parameter sweeping, a quantum state is found to still follow the eigenstate solution until it encounters the EPs, which can dramatically alter the tunneling process, leading to breakdown of adiabaticity. The EPs can be formed and changed by both nonreciprocity and nonlinearity parameters. The competition between nonreciprocity and nonlinearity yields rich pictures of adiabatic quantum evolutions. However, in the strong nonreciprocity regime, the nonlinear interaction effect is completely suppressed, and the nonzero adiabatic tunneling probabilities are analytically deduced in an explicit form and found to be independent of nonlinear interactions. An explicit phase diagram of adiabaticity for a large range of nonreciprocity and nonlinearity parameters is obtained. Our work provides a non-Hermitian extension of the celebrated LZT model, achieves insight into the adiabatic evolution of the non-Hermitian system, and might stimulate further explorations of the non-Hermitian topological properties in both theory and experiment.

### ACKNOWLEDGMENTS

We are grateful to Difa Ye and Bin Sun for valuable suggestions and discussions. This work was supported by the National Natural Science Foundation of China (Contract No. 12005173), the Natural Science Foundation of Gansu Province (Contract No. 20JR10RA082), the China Postdoc-



toral Science Foundation (Contract No. 2020M680318), and

the NSAF (Contract No. U1930402, No. U1930403).

- 
- [1] L. D. Landau, *Phys. Z. Sowjetunion* **2**, 46 (1932).
  - [2] C. Zener, *Proc. R. Soc. London, Ser. A* **137**, 696 (1932).
  - [3] M. Sillanpää, T. Lehtinen, A. Paila, Y. Makhlin, and P. Hakonen, *Phys. Rev. Lett.* **96**, 187002 (2006).
  - [4] S. Ashhab, J. R. Johansson, and F. Nori, *Phys. Rev. A* **74**, 052330 (2006).
  - [5] D. M. Berns, M. S. Rudner, S. O. Valenzuela, K. K. Berggren, W. D. Oliver, L. S. Levitov, and T. P. Orlando, *Nature* **455**, 51 (2008).
  - [6] G. D. Fuchs, V. V. Dobrovitski, D. M. Toyli, F. J. Heremans, and D. D. Awschalom, *Science* **326**, 1520 (2009).
  - [7] H. Ribeiro and G. Burkard, *Phys. Rev. Lett.* **102**, 216802 (2009).
  - [8] J. R. Petta, H. Lu, and A. C. Gossard, *Science* **327**, 669 (2010).
  - [9] R. Khomeriki and S. Ruffo, *Phys. Rev. Lett.* **94**, 113904 (2005).
  - [10] B. Wu and Q. Niu, *Phys. Rev. A* **61**, 023402 (2000).
  - [11] O. Zobay and B. M. Garraway, *Phys. Rev. A* **61**, 033603 (2000).
  - [12] J. Liu, L. Fu, B.-Y. Ou, S.-G. Chen, D.-I. Choi, B. Wu, and Q. Niu, *Phys. Rev. A* **66**, 023404 (2002).
  - [13] E. J. Mueller, *Phys. Rev. A* **66**, 063603 (2002).
  - [14] O. Morsch, J. H. Müller, M. Cristiani, D. Ciampini, and E. Arimondo, *Phys. Rev. Lett.* **87**, 140402 (2001).
  - [15] M. Cristiani, O. Morsch, J. H. Müller, D. Ciampini, and E. Arimondo, *Phys. Rev. A* **65**, 063612 (2002).
  - [16] J. Liu, B. Wu, and Q. Niu, *Phys. Rev. Lett.* **90**, 170404 (2003).
  - [17] M. Jona-Lasinio, O. Morsch, M. Cristiani, N. Malossi, J. H. Müller, E. Courtade, M. Anderlini, and E. Arimondo, *Phys. Rev. Lett.* **91**, 230406 (2003).
  - [18] D. Witthaut, E. M. Graefe, and H. J. Korsch, *Phys. Rev. A* **73**, 063609 (2006).
  - [19] B. Wu and J. Liu, *Phys. Rev. Lett.* **96**, 020405 (2006).
  - [20] K. Smith-Mannschott, M. Chuchem, M. Hiller, T. Kottos, and D. Cohen, *Phys. Rev. Lett.* **102**, 230401 (2009).
  - [21] A. Zenesini, C. Sias, H. Lignier, Y. Singh, D. Ciampini, O. Morsch, R. Mannella, E. Arimondo, A. Tomadin, and S. Wimberger, *New J. Phys.* **10**, 053038 (2008).
  - [22] A. Zenesini, H. Lignier, G. Tayebirad, J. Radogostowicz, D. Ciampini, R. Mannella, S. Wimberger, O. Morsch, and E. Arimondo, *Phys. Rev. Lett.* **103**, 090403 (2009).
  - [23] Y.-A. Chen, S. D. Huber, S. Trotzky, I. Bloch, and E. Altman, *Phys. Rev. Lett.* **7**, 61 (2011).
  - [24] C. Kasztelan, S. Trotzky, Y.-A. Chen, I. Bloch, I. P. McCulloch, U. Schollwöck, and G. Orso, *Phys. Rev. Lett.* **106**, 155302 (2011).
  - [25] F. A. An, E. J. Meier, J. Ang'ong'a, and B. Gadway, *Phys. Rev. Lett.* **120**, 040407 (2018).
  - [26] Y. Zhang, Z. Gui, and Y. Chen, *Phys. Rev. A* **99**, 023616 (2019).
  - [27] Q. Guan, M. K. H. Ome, T. M. Bersano, S. Mossman, P. Engels, and D. Blume, *Phys. Rev. Lett.* **125**, 213401 (2020).
  - [28] N. A. Sinitsyn, *Phys. Rev. B* **66**, 205303 (2002).
  - [29] A. V. Shytov, *Phys. Rev. A* **70**, 052708 (2004).
  - [30] M. V. Volkov and V. N. Ostrovsky, *J. Phys. B: At. Mol. Opt. Phys.* **37**, 4069 (2004).
  - [31] G.-F. Wang, D.-F. Ye, L.-B. Fu, X.-Z. Chen, and J. Liu, *Phys. Rev. A* **74**, 033414 (2006).
  - [32] N. A. Sinitsyn, *Phys. Rev. A* **87**, 032701 (2013).
  - [33] N. A. Sinitsyn, *Phys. Rev. A* **90**, 062509 (2014).
  - [34] S. Ashhab, *Phys. Rev. A* **94**, 042109 (2016).
  - [35] F. Li, C. Sun, V. Y. Chernyak, and N. A. Sinitsyn, *Phys. Rev. A* **96**, 022107 (2017).
  - [36] R. K. Malla and M. E. Raikh, *Phys. Rev. B* **96**, 115437 (2017).
  - [37] D. A. Garanin and R. Schilling, *Phys. Rev. B* **66**, 174438 (2002).
  - [38] F.-Q. Dou, J. Liu, and L.-B. Fu, *Phys. Rev. A* **98**, 022102 (2018).
  - [39] C. M. Bender and S. Boettcher, *Phys. Rev. Lett.* **80**, 5243 (1998).
  - [40] V. V. Konotop, J. Yang, and D. A. Zezyulin, *Rev. Mod. Phys.* **88**, 035002 (2016).
  - [41] L. Feng, R. El-Ganainy, and L. Ge, *Nat. Photon.* **11**, 752 (2017).
  - [42] M.-A. Miri and A. Alù, *Science* **363**, 6422 (2019).
  - [43] R. El-Ganainy, K. G. Makris, M. Khajavikhan, Z. H. Musslimani, S. Rotter, and D. N. Christodoulides, *Nat. Phys.* **14**, 11 (2018).
  - [44] Y. Ashida, Z. Gong, and M. Ueda, *Adv. Phys.* **69**, 249 (2020).
  - [45] E. J. Bergholtz, J. C. Budich, and F. K. Kunst, *Rev. Mod. Phys.* **93**, 015005 (2021).
  - [46] V. M. Akulin and W. P. Schleich, *Phys. Rev. A* **46**, 4110 (1992).
  - [47] Y. Avishai and Y. B. Band, *Phys. Rev. A* **90**, 032116 (2014).
  - [48] C. He and R. R. Jones, *Phys. Rev. A* **104**, 013111 (2021).
  - [49] D. L. Sounas and A. Alù, *Nat. Photon.* **12**, 774 (2017).
  - [50] M. Fruchart, R. Hanai, P. B. Littlewood, and V. Vitelli, *Nature* **592**, 363 (2021).
  - [51] Y. Castin and R. Dum, *Phys. Rev. Lett.* **79**, 3553 (1997).
  - [52] Y. Castin and R. Dum, *Phys. Rev. A* **57**, 3008 (1998).
  - [53] J. Liu, C. Zhang, M. G. Raizen, and Q. Niu, *Phys. Rev. A* **73**, 013601 (2006).
  - [54] W. P. Su, J. R. Schrieffer, and A. J. Heeger, *Phys. Rev. B* **22**, 2099 (1980).
  - [55] Z. Wang, Y. Chong, J. D. Joannopoulos, and M. Soljačić, *Nature* **461**, 772 (2009).
  - [56] X.-L. Qi and S.-C. Zhang, *Physics Today* **63**, 33 (2010).
  - [57] P. Lodahl, S. Mahmoodian, S. Stobbe, A. Rauschenbeutel, P. Schneeweiss, J. Volz, H. Pichler, and P. Zoller, *Nature* **541**, 473 (2017).
  - [58] K. Stannigel, P. Komar, S. J. M. Habraken, S. D. Bennett, M. D. Lukin, P. Zoller, and P. Rabl, *Phys. Rev. Lett.* **109**, 013603 (2012).
  - [59] J. Kim, M. C. Kuzyk, K. Han, H. Wang, and G. Bahl, *Nat. Phys.* **11**, 275 (2015).
  - [60] S. Barzanjeh, M. Aquilina, and A. Xuereb, *Phys. Rev. Lett.* **120**, 060601 (2018).
  - [61] H. Li, T. Kottos, and B. Shapiro, *Phys. Rev. Applied* **9**, 044031 (2018).
  - [62] Z. Gong, Y. Ashida, K. Kawabata, K. Takasan, S. Higashikawa, and M. Ueda, *Phys. Rev. X* **8**, 031079 (2018).
  - [63] D.-W. Zhang, Y.-Q. Zhu, Y. X. Zhao, H. Yan, and S.-L. Zhu, *Adv. Phys.* **67**, 253 (2018).
  - [64] W. Gou, T. Chen, D. Xie, T. Xiao, T.-S. Deng, B. Gadway, W. Yi, and B. Yan, *Phys. Rev. Lett.* **124**, 070402 (2020).
  - [65] M. Born, *Z. Phys.* **40**, 167 (1927).
  - [66] V. Born, M. and Fock, *Z. Phys.* **51**, 165 (1928).
  - [67] E. Farhi, J. Goldstone, S. Gutmann, and M. Sipser, "Quantum computation by adiabatic evolution," (2000), [arXiv:quant-ph/0001106](https://arxiv.org/abs/quant-ph/0001106).
  - [68] E. Farhi, J. Goldstone, S. Gutmann, J. Lapan, A. Lundgren, and D. Preda, *Science* **292**, 472 (2001).

- [69] T. Albash and D. A. Lidar, [Rev. Mod. Phys. \*\*90\*\*, 015002 \(2018\)](#).
- [70] D. Guéry-Odelin, A. Ruschhaupt, A. Kiely, E. Torrontegui, S. Martínez-Garaot, and J. G. Muga, [Rev. Mod. Phys. \*\*91\*\*, 045001 \(2019\)](#).
- [71] J. Liu and L. B. Fu, [Phys. Rev. A \*\*81\*\*, 052112 \(2010\)](#).
- [72] B. Wu, J. Liu, and Q. Niu, [Phys. Rev. Lett. \*\*94\*\*, 140402 \(2005\)](#).
- [73] H. Pu, P. Maenner, W. Zhang, and H. Y. Ling, [Phys. Rev. Lett. \*\*98\*\*, 050406 \(2007\)](#).
- [74] J. Liu, S. C. Li, L. B. Fu, and D. F. Ye, *Nonlinear Adiabatic Evolution of Quantum Systems. In: Nonlinear Adiabatic Evolution of Quantum Systems* (Springer, Singapore, 2018).
- [75] S. Ibáñez, S. Martínez-Garaot, X. Chen, E. Torrontegui, and J. G. Muga, [Phys. Rev. A \*\*84\*\*, 023415 \(2011\)](#).
- [76] Q. Zhang and B. Wu, [Phys. Rev. A \*\*99\*\*, 032121 \(2019\)](#).
- [77] T. Z. Luan, H. Z. Shen, and X. X. Yi, [Phys. Rev. A \*\*105\*\*, 013714 \(2022\)](#).
- [78] S. Eckel, J. G. Lee, F. Jendrzejewski, N. Murray, C. W. Clark, C. J. Lobb, W. D. Phillips, M. Edwards, and G. K. Campbell, [Nature \*\*506\*\*, 200 \(2014\)](#).
- [79] A. J. Lichtenberg and M. A. Lieberman, *Regular and Stochastic Motion* (Springer, Singapore, 1983).
- [80] L. D. Landau and E. M. Lifshitz, *Mechanics* (Pergamon, Oxford, 1977).